Onset of Turbulence in a Drift Wave–Zonal Flow System

Ryusuke NUMATA[1)], Rowena BALL[1,2)], Robert L. DEWAR[1)] and Linda. STALS[2)]

[1)] *Department of Theoretical Physics, Research School of Physical Sciences & Engineering, The Australian National University, Canberra, ACT 0200, Australia*

[2)] *Mathematical Sciences Institute, The Australian National University, Canberra, ACT 0200, Australia*

Numerical analyses of bifurcation phenomena in the Hasegawa-Wakatani model are presented, that provide new insights into the interactions between turbulence and zonal flows in the tokamak plasma edge region. The simulation results show a regime where, after an initial transient, drift wave turbulence is suppressed through zonal flow generation. As a parameter controlling the strength of the turbulence is tuned, this zonal-flow-dominated state is rapidly destroyed and a turbulence-dominated state re-emerges. The transition is explained in terms of the Kelvin-Helmholtz stability of zonal flows. This is the first observation of an upshift of turbulence onset in the resistive drift wave system, which is analogous to the well-known Dimits shift in turbulence driven by ion temperature gradients.

Keywords: bifurcation, transition, drift wave, turbulence, zonal flow

1 Introduction

Fusion plasmas and other turbulent flows in quasi-two-dimensional (2D) geometry can undergo spontaneous transitions to a turbulence-suppressed regime. Known as *L–H* (low-to-high confinement) transitions in plasmas, they are studied intensively because confinement enhancement may supervene through the concomitant abatement of anomalous or turbulent particle and heat fluxes. In tokamak edge plasmas *L–H* transitions are associated with nonlinearly self-generated poloidal $\boldsymbol{E} \times \boldsymbol{B}$ shear or zonal flows, which absorb energy from drift waves and consume the small scale eddies that mediate turbulent transport. It is now widely accepted that control of emergent zonal flows is crucial to achieving and sustaining improved confinement [1].

In this paper we present the results of analytic and numerical investigations of transitions between turbulence-dominated and zonal-flow-dominated regimes, using the Hasegawa–Wakatani (HW) model [2, 3] for electrostatic resistive drift wave turbulence in 2D slab geometry. We find that bifurcations in the model correspond to the onset of drift wave driven turbulence, generation of zonal flows, and re-emergence of drift wave turbulence as the zonal flows become unstable. This latter phenomenon is analogous to the Dimits shift [4] described for turbulence driven by ion temperature gradients (ITG).

2 Hasegawa–Wakatani model

The physical setting of the HW model may be considered as the edge region of a tokamak plasma of nonuniform density $n_0 = n_0(x)$ and in a constant equilibrium magnetic field $\boldsymbol{B} = B_0 \nabla z$. Following the drift wave ordering [5], the ion vorticity $\zeta \equiv \nabla^2 \varphi$ (φ is the electrostatic potential, $\nabla^2 = \partial^2/\partial x^2 + \partial^2/\partial y^2$ is the 2D Laplacian) and the density fluctuations n are governed by the equations

$$\frac{\partial}{\partial t}\zeta + \{\varphi, \zeta\} = \alpha(\varphi - n) - D\nabla^4 \zeta, \tag{1}$$

$$\frac{\partial}{\partial t}n + \{\varphi, n\} = \alpha(\varphi - n) - \kappa \frac{\partial \varphi}{\partial y} - D\nabla^4 n, \tag{2}$$

where $\{a, b\} \equiv (\partial a/\partial x)(\partial b/\partial y) - (\partial a/\partial y)(\partial b/\partial x)$ is the Poisson bracket, D is the dissipation coefficient. The background density is assumed to have an unchanging exponential profile: $\kappa \equiv (\partial/\partial x) \ln n_0$. Electron parallel motion is determined by Ohm's law with electron pressure $p_\mathrm{e} = nT_\mathrm{e}$,

$$j_z = -env_{\mathrm{e},z} = -\frac{1}{\eta}\frac{\partial}{\partial z}\left(\varphi - \frac{T_\mathrm{e}}{e}\ln n\right), \tag{3}$$

assuming electron temperature T_e to be constant (isothermal electron fluid). This relation gives the coupling between ζ and n through the adiabaticity operator $\alpha \equiv -T_\mathrm{e}/(\eta n_0 \omega_\mathrm{ci} e^2)\partial^2/\partial z^2$ appearing in Eqs. (1) and (2). In our 2D setting α becomes a constant coefficient when acting on the drift wave components of φ and n by the replacement $\partial/\partial z \to \mathrm{i}k_z$, where $2\pi/k_z = L_\parallel \gg L_y$ is a length characteristic of the drift waves' phase variation along the field lines. However, since zonal components of fluctuations ($k_y = k_z = 0$ modes) do not contribute to the parallel current, this resistive coupling term must be modified with care [6]. Recalling that turbulence in the tokamak edge region, where there is strong magnetic shear, is considered here, $k_y = 0$ should always coincide with $k_z = 0$ because any potential fluctuation on the flux surface is neutralized by parallel electron motion. Let us define zonal and non-zonal components of a variable f as

$$\text{zonal: } \langle f \rangle = \frac{1}{L_y}\int f \mathrm{d}y, \quad \text{non-zonal: } \tilde{f} = f - \langle f \rangle,$$

author's e-mail: ryusuke.numata@anu.edu.au

where L_y is the periodic length in y, and remove the contribution by the zonal components in the resistive coupling term in Eqs. (1) and (2). Subtraction of the zonal components from the resistive coupling term $\alpha(\varphi - n) \to \alpha(\tilde{\varphi} - \tilde{n})$ yields the modified HW (MHW) equations,

$$\frac{\partial}{\partial t}\zeta + \{\varphi, \zeta\} = \alpha(\tilde{\varphi} - \tilde{n}) - D\nabla^4\zeta, \tag{4}$$

$$\frac{\partial}{\partial t}n + \{\varphi, n\} = \alpha(\tilde{\varphi} - \tilde{n}) - \kappa\frac{\partial\varphi}{\partial y} - D\nabla^4 n. \tag{5}$$

The variables in Eqs. (4) and (5) have been normalized by

$$x/\rho_\mathrm{s} \to x, \;\; \omega_\mathrm{ci}t \to t, \;\; e\varphi/T_\mathrm{e} \to \varphi, \;\; n_1/n_0 \to n,$$

where $\rho_\mathrm{s} \equiv \sqrt{T_\mathrm{e}/m}\omega_\mathrm{ci}^{-1}$ is the ion sound Larmor radius ($v_\mathrm{si} \equiv \sqrt{T_\mathrm{e}/m}$ is the ion sound velocity in the cold ion limit), n_1 is the fluctuating part of the density.

Wakatani and Hasegawa found [3] that excitations of waves having k_z that maximizes the linear growth rate (for given k_x and k_y) are most likely to occur, since the plasma can choose any parallel wavenumber (k_z). Using the parallel wave number of the maximum growth rate, α is given by $\alpha = 4k^2 k_y\kappa/(1 + k^2)^2$. This also gives $\alpha = 0$ for the zonal mode.

The MHW model spans two limits with respect to the adiabaticity parameter α. In the adiabatic limit $\alpha \to \infty$ (collisionless plasma), the non-zonal component of electron density obeys the Boltzmann relation $\tilde{n} = n_0(x)\exp(\tilde{\varphi})$, and the equations are reduced to the Hasegawa–Mima equation [5]. In the hydrodynamic limit $\alpha \to 0$, the equations are decoupled. The vorticity is determined by the 2D Navier-Stokes equation, and the density becomes a passive scalar. The advantage of our choice of α as a free parameter is the capability for treating the limits in a unified manner.

In the adiabatic, ideal limit ($\alpha \to \infty$, $D \to 0$) the MHW system has two dynamical invariants, the energy E and the potential enstrophy W,

$$E = \frac{1}{2}\int(n^2 + |\nabla\varphi|^2)\mathrm{d}\boldsymbol{x}, \quad W = \frac{1}{2}\int(n - \zeta)^2\mathrm{d}\boldsymbol{x}, \tag{6}$$

where $\mathrm{d}\boldsymbol{x} = \mathrm{d}x\mathrm{d}y$, which constrain the fluid motion. Conservation laws are given by

$$\frac{\mathrm{d}E}{\mathrm{d}t} = \Gamma_n - D_\alpha - D_E, \quad \frac{\mathrm{d}W}{\mathrm{d}t} = \Gamma_n - D_W, \tag{7}$$

where fluxes and dissipations are given by

$$\Gamma_n = -\kappa\int\tilde{n}\frac{\partial\tilde{\varphi}}{\partial y}\mathrm{d}\boldsymbol{x},$$

$$D_\alpha = \alpha\int(\tilde{n} - \tilde{\varphi})^2\mathrm{d}\boldsymbol{x},$$

$$D_E = D\int((\nabla^2 n)^2 + |\nabla\zeta|^2)\mathrm{d}\boldsymbol{x},$$

$$D_W = D\int(\nabla^2 n - \nabla^2\zeta)^2\mathrm{d}\boldsymbol{x}.$$

Unlike the Hasegawa–Mima model which is an energy-conserving system, the MHW model has an energy source Γ_n. Due to the parallel resistivity, $\tilde{n}$ and $\tilde{\varphi}$ can fluctuate out of phase which produces non-zero Γ_n. The system can absorb free energy contained in the background density profile through the resistive drift wave instability.

3 Simulation Results

The MHW equations are solved in a doubly periodic square slab domain with box size $L = 2\pi/\Delta k$ where the lowest wavenumber $\Delta k = 0.15$ ($L \sim 42$). The equations are discretized on 256×256 grid points by the finite difference method. We examine the effects of the parameters κ and α on the nonlinearly saturated state, and fix $D = 10^{-4}$ throughout this paper.

We start simulations by imposing small amplitude random perturbations. The perturbations grow linearly in the initial phase and generate drift waves, then the drift waves undergo secondary instabilities which excite zonal flows until nonlinear saturation occurs. In the saturated state, we observe that $\Gamma_n \simeq D_\alpha \gg D_E, D_W$. The spatial structure of the saturated electrostatic potential is shown in Fig. 1. We observe that zonally elongated structures of the electrostatic potential are generated in the MHW model because the modification removes the unphysical resistive dissipation of the zonal modes. The zonal flows carry nearly all the kinetic energy in the final state — they have absorbed nearly all the energy from the drift waves. The build-up of the zonal flow and resulting transport suppression highlight the importance of the modification of the model in the nonlinear regime [7].

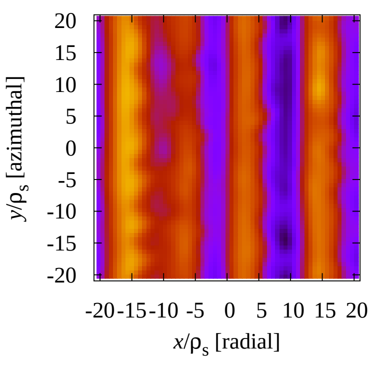

Fig. 1 Contour plot of φ in the saturated state. Zonally elongated structure of the electrostatic potential is clearly visible in the MHW model.

Let us show how the parameters affect the saturated state in the MHW model. In Fig. 2, we plot the ratio of the kinetic energy of the zonal flow ($F \equiv 1/2\int(\partial\langle\varphi\rangle/\partial x)^2\mathrm{d}\boldsymbol{x}$)

to the total kinetic energy ($E^k \equiv 1/2 \int |\nabla\varphi|^2 \mathrm{d}\boldsymbol{x}$) against α. It is clearly seen that there are two types of saturated states: one where zonal flows prevail and the other dominated by isotropic turbulence. Conversion from one state to the other occurs over a narrow range of the parameter space. We can see that zonal flows are generated in the adiabatic regime ($\alpha \gg 1$) while isotropic flows are generated in the hydrodynamic regime ($\alpha \ll 1$). Transition to the turbulent state also occurs if the drift wave instability is driven strongly by increasing the density gradient parameter κ.

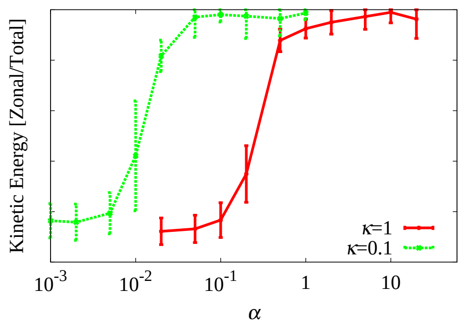

Fig. 2 Parameter dependence of the zonal kinetic energy normalized by the total kinetic energy. Transitions from a zonal-flow-dominated state to a turbulence-dominated state occur.

4 Stability of Zonal Flow

We examine the stability of the zonal flows obtained from the numerical simulations, and compare the stability threshold and the transition point in this section. We consider the perturbation around the zonal flow background. The electrostatic potential and the density are decomposed as $\varphi = \varphi_0(x) + \hat{\varphi}(x) \exp \mathrm{i}(k_y y - \omega t)$, and $n = \hat{n}(x) \exp \mathrm{i}(k_y y - \omega t)$ where $\mathrm{d}\varphi_0/\mathrm{d}x = V$ gives the background flow in the y direction. By linearizing the MHW equations, we obtain an eigenvalue equation containing the effect of κ and α,

$$\left[\frac{\mathrm{d}^2}{\mathrm{d}x^2} - k_y^2 + \frac{k_y V''}{\omega - k_y V}\right]\hat{\varphi} - \frac{\mathrm{i}\alpha}{\omega - k_y V + \mathrm{i}\alpha}\left(1 - \frac{k_y \kappa}{\omega - k_y V}\right)\hat{\varphi} = 0. \quad (8)$$

We neglect the viscosity. The generated zonal flows in the y direction are assumed to have a sinusoidal profile, $V = V_0 \sin(\lambda x)$. The amplitude V_0 and wavenumber $\lambda = n_\lambda \pi / L$ are determined from the simulation results as $V_0 \propto \kappa^2$, and $\lambda \approx 0.3$. We solve the eigenvalue equation by the standard shooting method in the domain $\mathcal{D} = \{x | -L/2 \leq x \leq L/2\}$. The boundary is assumed to be rigid $\hat{\varphi}(\pm L/2) = 0$ for simplicity.

In two limits ($\alpha \to 0$ and $\alpha \to \infty$), some conditions for stability are known (see [8] and references therein), and the eigenvalue problem is rather simple because it is not necessary to consider the continuous spectra on the real ω axis. If we find the eigenvalue ω and the corresponding eigenfunction $\hat{\varphi}$, the complex conjugate of ω is also an eigenvalue and the corresponding eigenfunction is given by the complex conjugate of $\hat{\varphi}$. Thus, we can always restrict our quest for eigenvalues in the upper half plane of the complex ω plane, and can neglect interactions between the point spectra and the continuous spectrum.

For the case of finite α the complex conjugate of an eigenvalue is not a eigenvalue, therefore we must solve for negative ω_i too. Moreover, there exist two continuous spectra in this case:

$$\omega = k_y V,\ k_y V - \mathrm{i}\alpha \quad \text{where } |V| \leq V_0. \quad (9)$$

Both represent convective transport due to the background flow. One of them is damped by the resistivity. These continua may interact with the point spectrum. Thus the situation is much more complicated in the intermediate α case compared with the adiabatic and hydrodynamic limits.

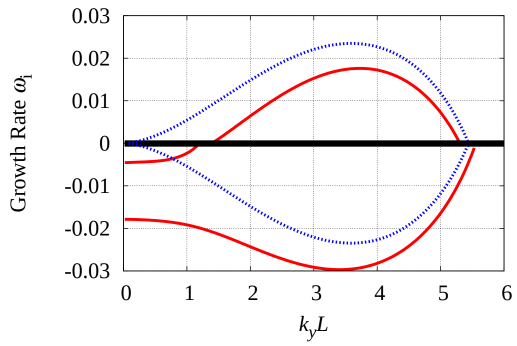

Fig. 3 Growth rates for HW case. Solid curves show the grawth rates for $\alpha = 0.0001$, and thick lines near the real ω axis denote two continuous spectra. Two branches from the $\alpha \to 0$ case (dotted line) are also shown for reference.

We first show the effect of α and neglect effect of κ. We consider $n_\lambda = 2$ for simplicity. Figure 3 shows the imaginary parts of the eigenvalues for $\alpha = 0.0001$. Two branches from the $\alpha \to 0$ case (dotted line) are also shown for reference, so that it is seen that ω_i is slightly shifted downwards for finite α. For increasing α, we observe the positive eigenvalues disappearing at $\alpha \approx 0.000417$.

Next, we consider the effect of κ in addition to α. Since κ always appears in the form of $\kappa\alpha$ and α is small in the vicinity of the threshold, the effect of κ is rather minor. κ does not significantly affect the behavior of the eigenvalues except that κ controls the amplitude of flow ($V_0 \propto \kappa^2$).

We summarize the stability of zonal flows by showing the bifurcation diagram in α-κ plane together with the numerically obtained results. The only excitable mode that can be resolved in the numerical simulation is the $k_y = 0.15$

mode, which is the first unstable mode of the primary instability (resistive drift wave instability). In Fig. 4, we show the stability threshold of $k_y = 0.15$ mode for the primary instability and the tertiary instability (KH instability). Each mark in the figure denotes a numerically obtained saturated state: ▲, ■, • represent respectively the zonal-flow-dominated, transitional, and turbulence-dominated states. In these states zonal flows contain more than 90%, 20-90%, and less than 20% of the total kinetic energy, respectively. The qualitative tendency of the thresholds in the bifurcation diagram shows agreement between the numerical simulations and the KH analysis, i.e. increasing α (κ) is stabilizing (destabilizing). Zonal-flow-dominated states are observed in between the primary and the tertiary instability thresholds. The emergence of a turbulent state is shifted from the primary threshold to the tertiary threshold due to the turbulence suppression effect of the zonal flow, which is analogous to the Dimits shift observed in ITG turbulence.

The reasons for the quantitative discrepancy between the boundary of the zonal and the turbulent states may be because of the simplification made in the KH analysis; the simplified flow profile, the boundary condition and viscosity may also affect the results.

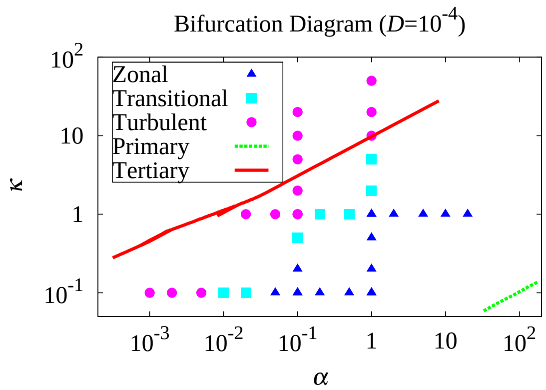

Fig. 4 Bifurcation diagram showing the correlation between the linearized stability estimates described in the text and the regimes observed in our turbulence simulations.

5 Conclusion

In summary, we have analyzed bifurcation phenomena in two-dimensional resistive drift wave turbulence. First, we have performed numerical simulations of the modified HW model to study bifurcation structures in a two-parameter (α-κ) space. We have shown that, in the MHW model, zonal flows are self-organized and suppress turbulence and turbulent transport over a range of parameters beyond the linear stability threshold for resistive drift waves. By performing a systematic parameter survey, we have found that such zonal-flow-dominated states suddenly disappear as a threshold is crossed, being replaced by a turbulence-dominated state.

The threshold of the onset of turbulence has been compared with the linear stability threshold of an assumed laminar zonal flow profile. Numerical analysis of the eigenvalue problem determining the stability of the assumed zonal flow profile in the HW model confirms the following trend: κ determines the amplitude of the zonal flows, thus, large κ destabilizes the zonal flows. On the other hand, the adiabatic response of parallel electrons given by α stabilizes them. The constructed bifurcation diagram in the α-κ plane for the HW model confirms the scenario of the onset of turbulence in the drift wave/zonal flow system being due to the disruption of zonal flows by KH instability.

Acknowledgments

The authors would like to acknowledge B. D. Scott for providing the simulation code used in this work. We thank P. N. Guzdar, W. Dorland, C. Tebaldi, and J. A. Krommes for useful discussions. This work is supported by the Australian Research Council.

[1] P. H. Diamond, S.-I. Itoh, K. Itoh, and T. S. Hahm, Plasma Phys. Control. Fusion **47**, R35 (2005).

[2] A. Hasegawa and M. Wakatani, Phys. Rev. Lett. **50**, 682 (1983).

[3] M. Wakatani and A. Hasegawa, Phys. Fluids **27**, 611 (1984).

[4] A. M. Dimits, G. Bateman, M. A. Beer, B. I. Cohen, W. Dorland *et al.*, Phys. Plasmas **7**, 969 (2000).

[5] A. Hasegawa and K. Mima, Phys. Rev. Lett. **39**, 205 (1977).

[6] W. Dorland and G. W. Hammett, Phys. Fluids B **5**, 812 (1993).

[7] R. Numata, R. Ball, and R. L. Dewar, in *Frontiers in Turbulence and Coherent Structures*, eds. J. P. Denier and J. S. Frederiksen (World Scientific, Singapore, 2007), vol. 6 of *World Scientific Lecture Notes in Complex Systems*, pp. 431–442, Proceedings of the COSNet/CSIRO Workshop on Turbulence and Coherent Structures in Fluids, Plasmas and Nonlinear Media, Canberra, Australia, 10-13 January 2006.

[8] R. Numata, R. Ball, and R. L. Dewar, accepted for publication in Phys. Plasmas (2007).